Sub-mm Wave Thermal Radiation from Silicon Wafers

Laurens F.E. Beijnen, Juan Bueno, Paolo Sberna, Marco Spirito, Andrea Neto

Delft University of Technology, Microelectronics, THz Sensing Group, The Netherlands
A.Neto@tudelft.nl

***Abstract* — The thermal energy radiated by silicon wafers with different conductivities is characterized experimentally in the mm and sub-mm wave ranges. These samples are heated up, and the energy that they radiate thermally is captured by different horn antennas covering the frequency band between 75 and 500 GHz. The measured thermal radiated power agrees with the prediction from Planck's law for the highly doped wafers, corresponding to high conductivities. However, for low conductivities, the measurements show a descending pattern as a function of the frequency, which is not in line with expectations from Planck's law. A recently developed theoretical model provides a classical explanation of these results [1].**

***Keywords* —radiometry, signal to noise ratio, noise equivalent power, silicon doping, zero bias detectors, THz.**

I. Introduction

According to radiometry, [2][3][4][5] the energy radiated by a body at given temperature T, and at a frequency f, can be estimated as the flux of the brightness $B(f,T)$ through a sphere surrounding the body at large distance. Assuming that the brightness is constant in all solid angle directions, the radiated spectral energy can be expressed, see eq. 30 from [3] as a function of the area S,

$$P(f) \approx 4\pi \cdot S \cdot B(f,T) \quad (1)$$

The brightness is expressed in terms of Planck's Black Body radiation law and proportional to the emissivity, a purely electromagnetic quantity. The experimental validation of Planck's law, after an exhaustive literature review, seems to be not complete. Crovini and Galgani [6] in 1984, pointed out that the experiments attempting a rigorous validation with known sources in the infrared and visible range date back to 1921, see [7]. On the other end the Cosmic Microwave Background radiation measurements, by Mather et al. in 1994, [8], dealt with remote sources with unknown characteristics including for their emissivity. For frequencies $hf \ll kBT$ (where $h \approx 6.6\,10^{-34}\,J\,s$ is the Planck's constant and $k_B \approx 1.38\,10^{-23}\,J/K$ is Boltzmann constant), Planck's law is approximated by the simpler Rayleigh-Jeans law, here expressed according to eq. 5 of [3] as

$$B(f,T) \approx 2\frac{k_B T}{\lambda_0^2} \cdot e_{mi}(f,T) \quad (2)$$

where $e_{mi}\,(f,T)$ is the frequency dependent emissivity and λ_0 indicates the free space wavelength. Eq. (2) is always used to describe the emission of bodies in the sub-THz regime. For instance, in [9] and [10], NIST proposes the use of specially designed water filled tanks, whose brightness is computed using eq. (2), as the reference for calibration of other sources. Another important application of eq. (2) is the calibration of radiometers for earth observation missions as reported in [11]. For silicon, to our knowledge, the only experimental validation of equation (2) has been conducted by Sato et al. [12] in 1967. Ravindra et al. [13] obtained a qualitative fit of the data from Sato using eq. (2) for measurements corresponding to high conductivities in 2001. However, no measurements have been ever reported for low conductivity semiconductors, and in the sub-THz spectrum.

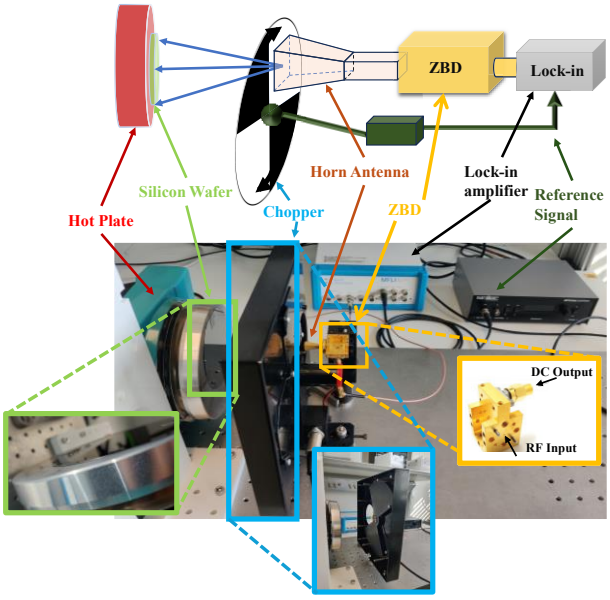

Fig. 1. Sketch of the measurement setup including the silicon wafer, the hot plate, the chopper, the horn antenna, the ZBD and the lock-in amplifier.

In this contribution, we present experiments that quantify the energy radiated in the sub-THz spectrum by crystalline silicon wafers, one of the semiconductors most widely used in the microelectronics industry. The results of the experiments should be simply predicted using (1)-(2) since the properties of crystalline silicon [14][15] are extremely well known and thus its emissivity. For high conductivity silicon (HCS), the measurements are in good agreement with Planck's law, as one would expect. However, the measurements associated with low conductivities, (LCS) can be surprising to the readers: as the frequency increases from the tens to the hundreds of GHz, the spectral energy radiated by silicon samples decreases. which is incongruent with Planck's law. An alternative, classical, explanation of the spectra is provided in paper [1], which stimulated this experimental study.

II. Experimental Setup

We present the experimental setup in this section. It is used to quantify the spectral energy radiated by silicon wafers, and consists of the generation of thermal radiation, the conversion of the thermal energy onto a chopped electrical signal, and the detection of this electrical signal.

A. Thermal radiation generation

Two different N-type (phosphorus doped), <100> orientation, CZ silicon wafers with thicknesses wz ranging from 300 μm to 600 μm and diameters $D_w = 10$ cm are used as thermal radiation sources. The main difference between these two wafers is their conductivity, one with high conductivity (0.001-0.005 Ω cm) and the other one with low conductivity (0.1 – 1 Ω cm). Although these conductivities are stated by the wafer supplier, the uncertainty is quite high. Thus, we decided to characterize them using our time domain THz spectroscopy system from Menlo [16], and fitting these measurements with the Drude's model, [17][18][19], of the conductivity. The conductivity can be expressed as $\sigma = \sigma_{qs}/(1 + j\omega\tau s)$ where $\sigma_{qs} = ne^2\tau_s/m_{eff}$, $e = 1.6\ 10^{-19}$ is the electron charge in Coulomb, m_{eff} is the effective mass of an electron in the silicon, which can be expressed in terms of the electron mass in free space as $m_{eff} = 0.26\ m_e$, and $m_e = 9.11\ 10^{-31}\ kg$. The fitting between the TDS measurement and the Drude model provided the scattering time, τ_s and concentration of free electrons, $n\ (el/m^3)$, i.e. the doping. Proceeding as discussed in [19] the real and imaginary parts of the refraction index are de-embedded. The results for the low conductivity silicon (LCS) are given as $\varepsilon_r = 11.7$, $\rho_{qs} = 1\ \Omega\ cm, n = 5\frac{10^{21}el}{m^3}, \tau_s = 1.87\ 10^{-13}s$.

In this work the sample LCS refers to two wafers of the same material stacked one on top of the other to obtain a unique sample of 600 μm thickness with a well-defined defined emissivity as explained in [20]. The silicon wafers are attached to an aluminum hot plate using Kapton tape. The temperature of the hot plate and therefore the silicon wafers is varied between 350 and 450 K in steps of 25 K.

B. Thermal to electrical energy conversion

The radiation emerging from the wafers is collected via directive, singly polarized horn antennas coupled to a Zero Bias Detector (ZBD) placed in front of the wafers at roughly 10 cm of distance. This can be seen in Fig. 1 where a sketch together with a picture of the setup is presented. We investigate the radiation coming from the wafers in a frequency range from 75 to 500 GHz, using four different horn antennas since each of the horns have a limited frequency bandwidth. We use a zero bias Schottky detectors from Virginia Diodes (VDI) [21] directly connected to the horn antenna as the receiver. The detectors take advantage of the low noise properties of Schottky barrier diodes [22][23], and are hosted in rectangular waveguide cavities that are directly connected to corresponding horns. The ZBDs are selected such that their frequency band matches the one of the horn antennas. Their properties are described in Table I, and a picture of one of them can be observed in one of the insets of Fig. 1.

Table 1. VDI Detector available [22].

Model	Frequency Band (GHz)	NEP ($pW/\sqrt{Hz}$)	Nominal Responsivity [V/(W Hz)]	Average Responsivity [V/(W Hz)]
WR10ZBD-F	75 – 110	3.5	2300	3381
WR5.1ZBD-F	140 – 220	4.3	1900	2399
WR3.4ZBD-F	220 – 330	4.8	1700	2317
WR2.2ZBD-F	330 - 500	6.8	1200	1638

The antenna horns are directly aiming at the center of the wafer, and their directivity (above 20 dBi's) is such that the wafer intercepts the main and the secondary side lobes of the horn antenna's pattern. The ZBD converts the THz energy into a DC signal. The DC signal output of the detector v^{DC} is proportional to the input power P_{in}^i via the responsivity of the ZBD R_{esp}:

$$v_i^{DC} = V_n + R_{esp}P_{in}^i \quad (3)$$

where V_n is the noise floor. The signal coming out from the silicon wafers is very small (in the order of pW), and ZBDs have a responsivity of 1000-2500 V/W (with an $NEP < -80\ dBm$), corresponding to detectable voltages in the tens of nV, which is a very small signal to detect. In order to enhance the sensitivity of our measurements, we connect the ZBDs to a lock-in amplifier from Zurich Instruments [24], which has a very low input noise. The lock-in is connected to an optical chopper [25], placed between the silicon wafers and the horn antennas.

C. Peculiarities of the experiment

The use of waveguide based detectors to characterize the thermal spectral energy radiated in the THz spectrum is not described in the scientific literature yet and thus a number of peculiarities (or difficulties) emerged that characterize these measurements:

1) The voltage signals in (3) signals are extremely small to the point that they cannot be read without an ad hoc read out. In our case it was decided to use the mentioned lock-in amplifier.

The VDI detectors have $NEP < -80\ dBm$, which corresponds to voltages in the tens of nV. These are the sensitivities needed for low thermal signals. Accordingly the dependence of the effective responsivity of the detectors from the instrument used to read out the voltage suggested us to connect the detectors to a lock-in amplifier from Zurich Instruments which has a very low input noise. If one were to plot the Fourier Transform (FT) of v^{DC}, even after the hot plate has been heated, he would obtain only noise. However, when the chopper is activated, the thermal signal is modulated and up converted to the chopper frequency, i.e. 32 Hz. The integration time of the scope was selected to be 18 seconds, the maximum in automatic mode. The notation $V^{FT}\ (t_i, 32\ Hz)$, indicates that this signal is a Fourier Transform, at 32 Hz, that is evaluated periodically at discrete intervals indicated as t_i . It is well known that the amplitude of

first harmonic of a square wave is proportional to the amplitude of the square harmonic itself by

$$v^{DC} = V^{FT}(t_i, 32\ Hz)\frac{\pi}{2} \quad (4)$$

Other points of attention were

2) The detectors were responsive out of the nominal band.
3) The responsivity of the detectors varies over the bands.
4) The hot plate is not able to maintain the temperature at a very precise value.

We characterized the above points as explained in [20].

III. Interpretation of the Voltage Readings

The next step is to establish the meaning of the voltage readings in terms of spectral energy so that useful information can be extracted. Given the described peculiarities of the experiment which already contribute some unavoidable errors, in the following interpretations details expected to contribute less than 5% have been neglected.

A. From voltage to measured spectral energies

For each $i-th$ measurement, with the $j\ -\ th$ detector the average voltage $v_{i,j}^{DC}$ is interpreted as the integration of a received $i\ -\ th$ energy spectral density, $E_{rec}^{i}(f)$, over the frequency band corresponding to the detector. Accordingly, one can express eq. (3) as,

$$v_{i,j}^{DC} = V_{n,j} + \int_{BW_j} R_{esp,j}(f) E_{rec}^{i}(f)\, df \quad (5)$$

Since all frequency harmonics associated to a thermal signal are imagined to be uncorrelated, the responsivity per unit BW would be the one specified in Table I. For simplicity one can assume that the responsivities and the energy spectra are uniform over the corresponding $j-th$ BW: so that

$$v_{i,j}^{DC} = V_{n,j} + BW_j\, R_{esp,j}\, E_{rec}^{i} \quad (6)$$

Assuming the noise negligible, the estimated spectral energy can be extracted from the measured voltages:

$$E_{rec}^{i} = \frac{v_{i,j}^{DC}}{R_{esp,j}\, BW_j} \quad (7)$$

B. Spectral Energies expected for single moded antennas

The energy, $E_{rec}^{i}(f)$ appearing in eq. (5) is the one acquired by the horn antennas and delivered to the detectors in each frequency band (after the out of band subtraction discussed in [20]). To compare it with simulations, one needs an expression for the expected energy. Using a few of the simplifications typically adopted in radiometry the incoherent energy received by a single moded antenna of assumed unitary efficiency can be expressed as [4]

$$E_{si}(f) \approx B(f,T)\frac{\lambda_0^2}{2} \quad (8)$$

where the antenna efficiency has been simplified to unity assuming negligible losses, congruently with the limited accuracy that can be reached in the campaign. To compare the results of modelling with the measurements one can use in (8) the expression of the brightness from eq. (2). One should note that eq. (2) is implicitly assuming that there is temperature equilibrium between the radiating body and the receiving one: they are both at the same temperature. However, in that situation there is no transfer of energy from one to the other. In the experiment described in this paper the transfer of energy occurs when the silicon is kept at temperatures higher than the detector: $T_{si} > T_{th}$.Accordingly the thermally induced transfer of energy can be described setting the spectral energy to

$$E_{si}(f, T_{si}) \approx k_B \Delta T\, e_{mi}(f, T_{si}) \quad (9)$$

where $\Delta T = T_{si} - T_{th}$. In the next section we plot the measured differential energy spectrum as eq. (7), compared with eq. (9). The emissivity $e_{mi}(f, T_{si})$ of the silicon wafers (LCS and HCS) is described in [20].

IV. Measured Spectral Energies

A. High conductivity silicon (HCS)

We start with the high conductivity one, which has a nominal resistivity indicated by the provider in the range $\rho \in (1 \rightarrow 5)10^{-5}\Omega - m$ corresponding to doping in the range $n \in (8 \rightarrow 1)10^{25} el/m^3$. The thickness of the wafer was 525 μm. These conductivities and doping correspond to emissivity well below 0.1, due to the silicon being very reflective. We heat up the wafer up to 475 K, while the ZBD appears to be at a temperature of 315 K. The energy received by the ZBDs in all four different bands when the silicon wafer is at 475 K can be seen in Fig. 2. The results of the measurements can be best matched by setting the trial doping to $n_{trial} = 0.65\ 10^{25}$. The actual value of the best fitting trial doping is slightly outside the range indicated by the provider.

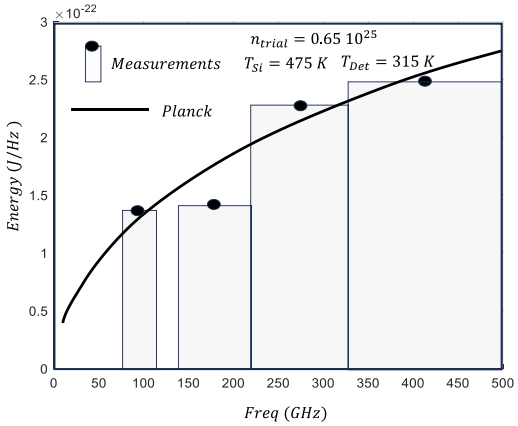

Fig. 2. Measured Spectral Energy Densities vs. predictions from Planck's law corrected with estimated emissivity for the estimated phosphorus doping of $n = 0.65\ 10^{25}$. Temperature of the silicon $T_{si} = 475\ K$ and temperature of the detector $T_{det} = 315K$.

However, considering that the levels of power received are at the limits of the sensitivity of the detectors, the frequency dependence of the calculation and the measurements is extremely good. For high conductivity silicon, a growing

spectral energy as a function of the frequency is predicted also by the companion work in [1].

B. Low conductivity silicon (LCS)

The story is completely different for lower doping corresponding to lower conductivity. The simulated spectral energy, is presented in Fig.3 for the case of the sample LCS. In Fig.3 it is compared with the measurement done when the hot plate was set to $T_{si} = 425K$.

The simulated curves correspond to a trial doping taken to be $n = 5\ 10^{21}$, while the thickness of the sample was $600\ \mu m$. However, it is evident that no choice of doping or thickness would ensure that the frequency dependence of the estimated spectral energy would match the frequency decreasing behaviour of the measurements. Fig.3, presents the results for the LCS wafer focusing on the spectral details for frequencies up to 500 GHz. It should be noted that for the low conductivity the measured energies are much higher, and thus the results more accurate, than for the high conductivity case. In this case the emissivity is systematically higher than 0.6, see [20].

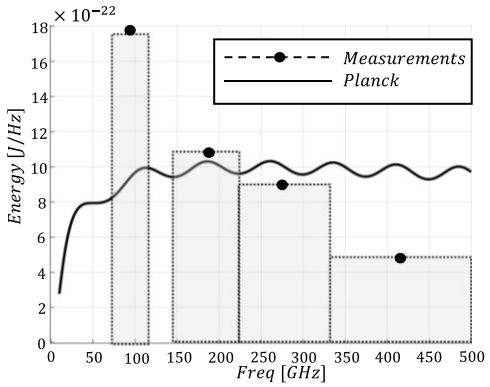

Fig. 3. Measured Spectral Energy Densities vs. predictions from Planck's law corrected with estimated emissivity for the estimated phosphorus doping of $n = 5\ 10^{21}$. Temperature of the silicon $T_{si} = 425K$ and detector $T_{det} = 315K$.

V. Conclusions

A series of measurements were performed to quantify the thermal radiation from n doped silicon wafers. The measurements assess the absolute power detected according to the most sensitive commercially available detectors. The resulting spectral energies are in the order of magnitude that one would expect resorting to classic radiometric procedures based on Planck's law and emissivities. When the doping of the wafer corresponds to high conductivity the received energy is small because of the high reflectivity of the wafer and presents a small growth as a function of the frequency. A credible trial doping value can be identified so that Planck's law, mediated by the emissivity, is in good agreement with the measurements. However, for lower doping and corresponding lower conductivities, when the energy received is much higher, the measurements strongly disagree with the predictions of Planck's law for any trial doping. The radiation intensity is clearly diminishing as a function of the frequency for all temperatures.

References

[1] A. Neto, "A Classical Electromagnetic Model for Thermal Emission from Ohmic Materials," European Conference on Antennas and Propagation 2023.

[2] Planck, " The Theory of Heat Radiation" (1906)

[3] G. Bekefi, and Sanborn C. Brown "Emission of Radio-Frequency Waves from Plasmas" American Journal of Physics 29, 404 (1961);

[4] Fawwaz T. Ulaby, Richard K. Moore, Adrian K. Fung, "Microwave remote sensing: active and passive volume 1: microwave remote sensing fundamentals and radiometry"; The Artech House Remote Sensing Library

[5] S. van Berkel, O. Yurduseven, A. Freni, A. Neto and N. Llombart, "THz Imaging Using Uncooled Wideband Direct Detection Focal Plane Arrays," in IEEE Transactions on Terahertz Science and Technology, vol. 7, no. 5, pp. 481-492, Sept.2017,doi: 10.1109/TTHZ.2017.2736338

[6] L. Crovini, L. Galgani "On the Accuracy of the Experimental Proof of Planck's Radiation Law"; Letere al Nuovo Cimento Vol. 39, No.. 10, 10 Marzo 1984:

[7] Rubens H and Michel G 1921 Prufung der Planckschen Strahlung Strahlungsformel Z. Phys. 22 569

[8] Mather, John C., et al. "Measurement of the cosmic microwave background spectrum by the COBE FIRAS instrument." The Astrophysical Journal, Part 1 (ISSN 0004-637X), vol. 420, no. 2, p. 439-444 420 (1994): 439-444.

[9] Z. Popovic and E. N. Grossman, "THz Metrology and Instrumentation," in IEEE Transactions on Terahertz Science and Technology, vol. 1, no. 1, pp. 133-144, Sept. 2011, doi: 10.1109/TTHZ.2011.2159553

[10] Charles Dietlein, Zoya Popović, and Erich N. Grossman, "Aqueous blackbody calibration source for millimeter-wave/terahertz metrology," Appl. Opt. 47, 5604-5615 (2008)

[11] G. Virone et al., "Thermal Vacuum Cold Target for the Metop SG MicroWave Imager," in IEEE Journal of Selected Topics in Applied Earth Observations and Remote Sensing, vol. 14, pp. 10348-10356, 2021,

[12] Tsutomu Satō "Spectral Emissivity of Silicon", Japanese Journal of Applied Physics, Volume 6, Number 3, 19967

[13] N.M.Ravindra, et al. "Emissivity Measurements and Modeling of Silicon-Related Materials: An Overview" International Journal of Thermophysics, Vol. 22, No. 5, September 2001

[14] D. B. M. Klaasen, "A unified mobility model for device simulation – I. Model equations and concentration dependence," Solid State Electron., vol. 35,no. 7, pp. 953–959, 1992.

[15] https://www.pvlighthouse.com.au

[16] "TERA K15 all fiber-coupled terahertz spectrometer," Menlo Systems. https://www.menlosystems.com/products/thz-time-domain-solutions/terak15 -terahertz-spectrometer/

[17] P. Drude, "Zur Elektronentheorie der Metalle", Annalen der Physik, Vol. 306, pp. 566613, Mar. 1900

[18] M. Dressel, M. Scheffler, "Verifying the Drude response", Annalen der Physik, 15, No. 78): 535544. 2006

[19] R. M. van Schelven, A. Fiorellini Bernardis, P. Sberna and A. Neto, "Drude Dispersion in the Transmission Line Modeling of Bulk Absorbers at Sub-mm Wave Frequencies: A Tool for Absorber Optimization," in IEEE Antennas and Propagation Magazine, to appeaar in Febrary 2022. doi: 10.1109/MAP.2021.3073092.

[20] L.F.E. Beijnen, J. Bueno, Y. Chen, P. Sberna, M. Spirito and A. Neto, "The THz Catastrophe. Part 1: Discrepancy Between Planck's Law and Experiments on Silicon Wafers," TechRxiv. June 03, 2024.

[21] Virginia Diodes,ZBD, https://www.vadiodes.com/en/products/detectors

[22] J. L. Hesler and T. W. Crowe, "NEP and responsivity of THz zero-bias Schottky diode detectors," 2007 Joint 32nd International Conference on Infrared and Millimeter Waves and the 15th International Conference on Terahertz Electronics, Cardiff, UK, 2007, pp. 844-845, doi: 10.1109/ICIMW.2007.4516758.

[23] L. Liu, J. L. Hesler, H. Xu, A. W. Lichtenberger and R. M. Weikle, "A Broadband Quasi-Optical Terahertz Detector Utilizing a Zero Bias Schottky Diode," in IEEE Microwave and Wireless Components Letters, vol. 20, no. 9, pp. 504-506, Sept. 2010, doi: 10.1109/LMWC.2010.2055553

[24] https://www.zhinst.com/europe/en/products/mfli-lock-in-amplifier

[25] https://scitec.uk.com/optical_chopper/